THE UNIVERSITY of EDINBURGH

Edinburgh Research Explorer

Role of convection in determining the budget of odd hydrogen in the upper troposphere

Citation for published version:
Collins, WJ, Stevenson, DS, Johnson, CE & Derwent, RG 1999, 'Role of convection in determining the budget of odd hydrogen in the upper troposphere' Journal of Geophysical Research, vol 104, no. D21, pp. 26927-26941., 10.1029/1999JD900143

Digital Object Identifier (DOI):
10.1029/1999JD900143

Link:
Link to publication record in Edinburgh Research Explorer

Document Version:
Publisher final version (usually the publisher pdf)

Published In:
Journal of Geophysical Research

Publisher Rights Statement:
Published in Journal of Geophysical Research: Atmospheres by the American Geophysical Union (1999)

General rights
Copyright for the publications made accessible via the Edinburgh Research Explorer is retained by the author(s) and / or other copyright owners and it is a condition of accessing these publications that users recognise and abide by the legal requirements associated with these rights.

Take down policy
The University of Edinburgh has made every reasonable effort to ensure that Edinburgh Research Explorer content complies with UK legislation. If you believe that the public display of this file breaches copyright please contact openaccess@ed.ac.uk providing details, and we will remove access to the work immediately and investigate your claim.

Download date: 20. Feb. 2015

JOURNAL OF GEOPHYSICAL RESEARCH, VOL. 104, NO. D21, PAGES 26,927-26,941, NOVEMBER 20, 1999

Role of convection in determining the budget of odd hydrogen in the upper troposphere

W. J. Collins, D. S. Stevenson, C. E. Johnson, and R. G. Derwent

Hadley Centre for Climate Research and Prediction, Meteorological Office, Bracknell, U.K.

Abstract. This paper presents a model study of the changes in upper tropospheric HO_x (=OH+HO_2) due to upward convective transport of surface pollutants. The model used is a three-dimensional global Lagrangian tropospheric chemistry transport model of 70 chemical species and 150 reactions including nonmethane hydrocarbon chemistry. It is driven by meteorological data from the U.K. Meterological Office with a 6 hour time resolution. We find that the effect of convection is to increase upper tropospheric (300–200 hPa) HO_x globally by over 50%. The effect is greatest over the tropical continents where convection and VOC emissions from vegetation are colocated. The convection of isoprene, and hydroperoxides has the greatest effect. Convecting formaldehyde and acetone has a lesser effect. The contribution from isoprene depends more on the convection of its degradation products than the convection of isoprene itself. The upper tropospheric HO_x budget is shown to be very sensitive to the model implementation of convective wet deposition.

1. Introduction

The importance of the odd hydrogen species HO_x (=OH+HO_2) in the photochemistry of the lower atmosphere, driven by the photolysis of ozone (O_3) and formaldehyde (HCHO) was identified by *Levy* [1971]. *Crutzen* [1974] established the link between the fast photochemistry of the odd hydrogen species and the life cycle of tropospheric ozone through the reactions of the HO_x species with the oxides of nitrogen, carbon monoxide (CO), and methane (CH_4). Understanding of the tropospheric HO_x budget was further extended by *Zimmerman et al.* [1978], who pointed out the potential importance of isoprene (C_5H_8) photo-oxidation as a formaldehyde source, in addition to that from methane photo-oxidation.

The tropospheric odd hydrogen budget has changed little in basic structure in the intervening two decades though considerable refinement has taken place driven by the improvements in theoretical modeling [*Crutzen and Fishman*, 1977; *Derwent and Curtis*, 1977; *Mahlman et al.*, 1980; *Jacob and Wofsy*, 1988; *Crutzen and Zimmerman*, 1991; *Lelieveld and Crutzen*, 1994; *Penner et al.*, 1991; *Kasibhatla et al.*, 1993]. The tropospheric odd hydrogen budget is now the subject of much research interest which has been stimulated by the availability of sophisticated, high quality observations of the major HO_x species in the upper troposphere, the hydroxyl (OH) and hydroperoxy (HO_2) radicals. These recent measurements [*Folkins et al.*, 1997; *Brune et al.*, 1998; *Wennberg et al.*, 1998] require a significantly greater odd hydrogen source than had been expected in the upper troposphere. A number of potential explanations have been advanced, invoking additional odd hydrogen carriers and additional atmospheric processes, such as convection. *Prather and Jacob* [1997] and *Jaeglé et al.* [1997] found that as well as underpredicting HO_x, box models also underpredicted the concentrations of hydrogen peroxide and methyl hydroperoxide in the upper troposphere. When additional sources of peroxides were added to the models, they were able to get good agreement between calculated and observed HO_x concentrations. This upper tropospheric input was designed to account for the convective uplift of boundary layer air with high peroxide concentrations. The origins of these high concentrations was not discussed, nor the possibility that the upper tropospheric concentrations of peroxides might be influenced by convection of precursors (such as longer chain organic compounds) as well as convection of the peroxides themselves.

In this tropospheric chemistry modeling study, a global three-dimensional Lagrangian chemistry transport model has been used to describe the main features of the tropospheric odd hydrogen budget. We separate the rapid interconversion processes between OH, HO_2, and organic radicals from the main HO_x source and sink processes in the analysis of the tropospheric odd hydrogen budget. On this basis then, the main odd hydrogen source terms identified in our study are photolysis of ozone in the ultra-violet in the presence of water (1) and photolysis of carbonyls (2)

$$O_3 + h\nu + H_2O \rightarrow 2OH + O_2, \quad (1)$$

$$RCHO + h\nu \rightarrow R'O_2 + R''O_2. \quad (2)$$

Published in 1999 by the American Geophysical Union.

Paper number 1999JD900143.

The ozone photolysis source dominates everywhere except in the upper troposphere where it is too dry. The most important sinks of HO_x are HO_x+HO_x recombination (3) and reaction with NO_2 (4).

$$OH + HO_2 \rightarrow H_2O, \quad (3)$$

$$OH + NO_2 \rightarrow HNO_3. \quad (4)$$

The NO_2 reaction is only important in regions of very high NO_x concentrations, such as the boundary layer over industrial continents. Another HO_x+HO_x recombination reaction is HO_2+HO_2 →H_2O_2, but this is not a HO_x sink if the H_2O_2 is photolyzed as described below.

A number of odd hydrogen temporary reservoir species have been identified as controlling odd hydrogen sink process in the troposphere. These are hydrogen peroxide (H_2O_2) and the organic hydroperoxides (ROOH), and are formed by the combining of two peroxy radicals (reactions (5) and (6))

$$RO_2 + HO_2 \rightarrow ROOH, \quad (5)$$

$$HO_2 + HO_2 \rightarrow H_2O_2. \quad (6)$$

These species can simply recycle the odd hydrogen if they are photolyzed, or act as sinks if they are deposited or oxidized by OH attack. They have much longer lifetimes than the radical species, so they can effectively transport HO_x radicals around the troposphere. The fast interconversion processes between the HO_x species control the lifecycles, lifetimes, and distributions of a wide range of tropospheric trace gases, particularly NO_x, ozone, and hydrocarbons.

As part of our study, we will revisit the *Zimmerman et al.* [1978] hypothesis concerning the importance of isoprene photo-oxidation as a source of tropospheric odd hydrogen. The representation of isoprene photo-oxidation, in tropospheric chemistry models has been a difficult and complex compromise between basic understanding of the process involved and practical computer capacity. Many global chemistry transport models have simply neglected to include isoprene photo-oxidation and others have implemented simplified [*Paulson and Seinfeld*, 1992] or parameterized [*Stockwell et al.*, 1997] representations of isoprene chemistry. Much recent progress has been made in the understanding in laboratory systems of the details of the atmospheric chemistry of isoprene [*Carter and Atkinson*, 1996]. In this study, we have attempted to represent two of the main facets of the complex influence of isoprene on the tropospheric odd hydrogen budget. The first facet is the rapid conversion of isoprene into C_4 and C_3 multifunctional unsaturated and dicarbonyl compounds, and the second is the formation of organic hydroperoxides.

2. Model Description

The model used in this work is the U.K. Meteorological Office tropospheric 3-D chemistry transport model (STOCHEM). This model takes a Lagrangian approach by dividing the troposphere into 50,000 air parcels which are advected with a 3 hour time step using archived winds from the Meteorological Office Unified Model. These winds are 6-hourly instantaneous values, taken either from operational meteorological analyses ($\sim 1^\circ \times 1^\circ$ resolution) or from climate integrations ($\sim 3^\circ \times 3^\circ$ resolution).

Each parcel holds the concentrations of 70 chemical species including NO_x, O_3, OH, HO_2, PAN, and hydrocarbons. The hydrocarbons modeled are methane (CH_4), ethane (C_2H_6), ethene (C_2H_4), propane (C_3H_8), propene (C_3H_6), n-butane (C_4H_{10}), toluene ($CH_3C_6H_5$), o-xylene ($(CH_3)_2C_6H_4$), and isoprene (C_5H_8), along with their oxidation products such as peroxy radicals (RO_2), hydroperoxides (ROOH), and carbonyls (e.g., formaldehyde (HCHO), acetaldehyde (CH_3CHO), acetone (CH_3COCH_3), methyl glyoxal (CH_3COCHO), and methyl vinyl ketone ($CH_3COCHCH_2$). The chemical species react according to 174 photolytic and thermal reactions, with a 5 min chemistry time step. The resulting parcel concentrations are mapped to a $5^\circ \times 5^\circ \times 9$ level grid for output.

The physical processes included are emission, dry and wet deposition, convection, and subgrid scale mixing between parcels. Emissions can be into the boundary layer or three-dimensional (from aircraft and lightning). Their rates are give in Table 1. For a more detailed model description, see *Collins et al.* [1997]. Improvements to the model since that paper are described below.

2.1. Meteorological Fields

The meteorological fields used are now instantaneous values, available every 6 hours from a general circulation model (GCM). The data used in this paper are from the Hadley Centre's climate version of the Meteorological Office's Unified Model [*Johns et al.*, 1997]. These data are at a resolution of 3.75° longitude × 2.5° latitude on 19 unevenly spaced levels between the surface and 4.6 hPa. Note that this grid applies only to fields imported from the GCM. All other input and output data use the grid described in the preceding section.

2.2. Advection Scheme

Parcels are now advected using a Runge-Kutta fourth order method with a time step of 3 hours. Linear interpolation from the wind grid to the parcel position is used in the horizontal and in time, and a cubic interpolation is used in the vertical direction.

There is now no variance term in the wind fields, so random displacements are added to the parcel each time step based on globally constant diffusivities. The horizontal diffusivity K_H is chosen to be 1300 $m^2\ s^{-1}$ (5300 $m^2\ s^{-1}$ in the boundary layer) and the vertical diffusivity K_η is chosen to be $7 \times 10^{-11} s^{-1}$ (equivalent to 7×10^{-5}-1×10^{-3} $m^2\ s^{-1}$).

2.3. Chemistry

The main additions to the chemistry since the *Collins et al.* [1997] paper have been propane and acetone chemistry, organic hydroperoxide formation, DMS ox-

Table 1. Model Emissions

Species	Anthropogenic	Biomass	Vegetation	Soil	Oceans	Aircraft	Lightning	Other[a]
NO_x	21.0	8.0	...	5.6	...	0.5	5.0	...
Hydrogen	20.0	20.0	...	5.0	5.0	...	...	...
Carbon monoxide	425.0	500.0	75.0	...	50.0	...	...	...
Methane	155.0	40.0	...	...	10.0	...	...	260.0
Ethene	17.0	10.0	20.0	...	...	...	...	...
Ethane	6.0	6.5	3.5	...	...	...	...	...
Propene	21.0	5.0	20.0	...	...	...	...	...
Propane	6.5	12.0	2.0	...	0.5	...	...	...
n-butane	47.0	2.0	8.0	...	...	...	...	...
Isoprene	...	...	506.0	...	...	...	...	...
o-xylene	4.7	...	...	...	...	...	...	...
Toluene	14.0	...	...	...	...	...	...	...
Formaldehyde	1.0	5.0	...	...	...	...	...	...
Acetaldehyde	0.3	...	...	...	...	...	...	...
Acetone	3.0	...	40.0[b]	...	...	...	...	...

Emissions in Tg yr^{-1}, except NO_x and HNO_3, which are in Tg (N) yr^{-1}, and SO_2, which are in Tg (S) yr^{-1}.
[a]Includes paddys (60 Tg yr^{-1}), tundra (50 Tg yr^{-1}), wetlands (65 Tg yr^{-1}), termites (20 Tg yr^{-1}), and other animals (85 Tg yr^{-1}).
[b]Represents production from terpene oxidation. Emissions are distributed seasonally according to terpene emissions in the GEIA inventory.

idation, and aqueous phase SO_2 oxidation. The last two have only small effects on ozone and HO_x levels (mostly due to the aqueous H_2O_2+SO_2 reaction) and will not be discussed further. Of the new species that have been added, those of most importance to this study are HO_2NO_2, C_3H_8, $C_3H_7O_2$, CH_3COCH_3, $CH_3COCH_3O_2$, C_2H_5OOH, C_3H_7OOH, secC_4H_9OOH, OHC_5H_8OOH, and MVKOOH. The new reactions are listed in Tables 2 and 3.

Propane and acetone oxidation can produce ozone in the continental boundary layer, and when photolyzed, acetone can generate HO_x. Our model acetone emissions of 43 Tg yr^{-1} combined with our propane emissions of 21 Tg yr^{-1} give a total acetone production rate of 70 Tg yr^{-1}. This is almost twice as large as the 40 Tg yr^{-1} estimate of *Singh et al.* [1994]. Our acetone emissions from vegetation (40 Tg yr^{-1}) are too high since they assume acetone is a major product of terpene oxidation. This is likely to exaggerate the role of acetone in our model.

Formation of hydroperoxides generally reduces HO_x in the continental boundary layer. They can act as HO_x reservoirs, transporting HO_x to remote regions, or as HO_x sinks if they are removed from the atmosphere. The effects on the upper troposphere will be discussed further in later sections.

Reasonably realistic representations of the aspects of isoprene chemistry have been assembled into the global three-dimensional model with current best estimates of the spatial, seasonal, and diurnal variations in isoprene emissions [*Guenther et al.*, 1995]. The most important reactions in the model isoprene degradation scheme for the upper troposphere are listed below (we also include ozone and NO_3 attack in the model). Reaction (8) or (9) produces methyl vinyl ketone (MVK) which reacts via (11) or (12) to produce methyl glyoxal which can be photolyzed to radicals (13).

$$C_5H_8 \xrightarrow{OH,O_2} OHC_5H_8O_2 \quad (7)$$

$$OHC_5H_8O_2 \xrightarrow{NO,O_2} MVK+HCHO+NO_2+HO_2 \quad (8)$$

$$\xrightarrow{HO_2} HOC_5H_8OOH \xrightarrow{OH} MVK+HCHO+OH \quad (9)$$

$$MVK \xrightarrow{OH,O_2} MVKO_2 \quad (10)$$

Table 2. New Photolysis Reactions in the Chemistry Model

Species		Products	Rate
$CH_3COCH_3 + h\nu$	→	$CH_3CO_2 + CH_3O_2$	*Martinez et al.*, [1992]
$HO_2NO_2 + h\nu$	→	HO_2+NO_2	*DeMore et al.*, [1994]
$C_2H_5OOH + h\nu$	→	$CH_3CHO + HO_2 + OH$	as CH_3OOH
$C_3H_7OOH + h\nu$	→	$CH_3COCH_3 + HO_2 + OH$	as CH_3OOH
sec$C_4H_9OOH + h\nu$	→	$CH_3COC_2H_5 + HO_2 + OH$	as CH_3OOH
$HOC_5H_8OOH + h\nu$	→	$MVK + HO_2 + OH + HCHO$	as CH_3OOH
$MVKOOH + h\nu$	→	$CH_3COCHO + HO_2 + OH + HCHO$	as CH_3OOH

Table 3. New Reactions Used in the Chemistry Model

Reactants		Products	Rate Constant
$NO_2 + O^3P$	→	$NO + O_2$	$6.5 \times 10^{-12} \exp(120/T)$
$NO_2 + HO_2 + M$	→	$HO_2NO_2 + M$	*DeMore et al.*, [1994]
$HO_2NO_2 + M$	→	$NO_2 + HO_2 + M$	*DeMore et al.*, [1994]
$HO_2NO_2 + OH$	→	$NO_2 + H_2O + O_2$	$1.3 \times 10^{-12} \exp(380/T)$
$NO_3 + HO_2$	→	$OH + NO_2 + O_2$	3.6×10^{-12}
$CH_3OOH + OH$	→	$CH_3O_2 + H_2O$	$1.90 \times 10^{-12} \exp(190/T)$
$CH_3OOH + OH$	→	$HCHO + OH$	$1.0 \times 10^{-12} \exp(190/T)$
$OH + C_3H_8$	→	$C_3H_7O_2 + H_2O$	$1.50 \times 10^{-17} T^2 \exp(44/T)$
$C_3H_7O_2 + NO$	→	$NO_2 + HO_2 + CH_3COCH_3$	4.8×10^{-12}
$OH + CH_3COCH_3$	→	$CH_3COCH_2O_2 + H_2O$	$5.34 \times 10^{-18} T^2 \exp(-230/T)$
$NO + CH_3COCH_2O_2$	→	$NO_2 + CH_3COO_2 + HCHO$	5.3×10^{-12}
$CH_3O_2 + CH_3COCH_2O_2$	→	$HO_2 + CH_3COO_2 + 2HCHO$	1.2×10^{-12}
$C_3H_7O_2 + CH_3O_2$	→	$HCHO + 2HO_2 + CH_3COCH_3$	4.0×10^{-14}
$HO_2 + C_2H_5O_2$	→	$C_2H_5OOH + O_2$	$7.5 \times 10^{-13} \exp(700/T)$
$OH + C_2H_5OOH$	→	$CH_3CHO + OH$	1.0×10^{-11}
$HO_2 + C_3H_7O_2$	→	$C_3H_7OOH + O_2$	$1.92 \times 10^{-13} \exp(1250/T)$
$OH + C_3H_7OOH$	→	$CH_3COCH_3 + OH$	2.42×10^{-11}
$HO_2 + secC_4H_9O_2$	→	$secC_4H_9OOH + O_2$	$2.24 \times 10^{-13} \exp(1250/T)$
$OH + secC_4H_9OOH$	→	$CH_3COC_2H_5 + OH$	3.21×10^{-11}
$O_3 + C_5H_8$	→	MVK + products	$7.86 \times 10^{-15} \exp(-1913/T)$
$O_3 + MVK$	→	CH_3COCHO + products	$7.56 \times 10^{-16} \exp(-1521/T)$
$HOC_5H_8O_2 + HO_2$	→	$HOC_5H_8OOH + O_2$	$2.45 \times 10^{-13} \exp(1250/T)$
$HOC_5H_8OOH + OH + H_2O$	→	$OH + HCHO + MVK$	4.20×10^{-11}
$MVKO_2 + HO_2$	→	$MVKOOH + O_2$	$2.23 \times 10^{-13} \exp(1250/T)$
$MVKOOH + OH$	→	$OH + HCHO + CH_3COCHO$	5.77×10^{-11}
$CH_3COCHO + OH$	→	$CH_3COO_2 + CO$	1.72×10^{-11}
$CHOCHO + OH$	→	$HO_2 + 2CO$	1.14×10^{-11}

Rate coefficients are in molecules^{-1} cm^3 s^{-1}.

$$MVKO_2 \xrightarrow{NO,O_2} CH_3COCHO + HCHO + NO_2 + HO_2 \quad (11)$$

$$\xrightarrow{HO_2} MVKOOH \xrightarrow{OH} CH_3COCHO + HCHO + OH \quad (12)$$

$$CH_3COCHO \xrightarrow{h\nu,2O_2} CH_3COO_2 + HO_2 + CO. \quad (13)$$

Here $MVKO_2$ and MVKOOH are used as shorthand for $CH_3COCH(OH)CH_2O_2$ and $CH_3COCH(OH)CH_2OOH$.

2.4. Convection Scheme

The model convection scheme is unchanged from the previous model version. It uses convective diagnostics from the driving General Circulation Model. These are the heights of the cloud bases and tops, cloud cover, and precipitation rate. These parameters are used to derive probabilities for a Lagrangian parcel to be involved in convective transport. Within each grid square, each parcel below the cloud top is randomly designated (according to the above probability) as convected or not. Those that are convected have their chemical species uniformly redistributed among all the convected parcels below the cloud top within a $5° \times 5°$ grid square. The advection, convection and mixing schemes have been validated using ^{222}Rn as a tracer [*Stevenson* et al., 1998].

2.5. Wet Deposition

Soluble species are removed by wet deposition depending on the dynamic and convective precipitation rates, using altitude dependent coefficients from *Penner et al.* [1994]. The species deposited are HNO_3, N_2O_5, SO_2, HCHO, H_2O_2, and the organic hydroperoxides (ROOH). The higher organic hydroperoxides are given the same coefficients as methyl hydroperoxide (CH_3OOH).

Convective precipitation is a subgrid scale process, removing material efficiently over a narrow column. Our removal rate is modified by the algorithm of *Walton et al.* [1988] to take account of fractional precipitation area, using a fraction of 0.3. At present, we wet deposit soluble species from every parcel equally within the square covered by the precipitation data ($3.75° \times 2.5°$) regardless of whether that parcel is subject to convective mixing. This means that the convective wet deposition is not completely coupled to the convective transport scheme.

3. Model Results

The model was run for a year, preceded by a 4 month spin-up. Figure 1 shows the diurnally averaged upper tropospheric HO_x distribution for January in the re-

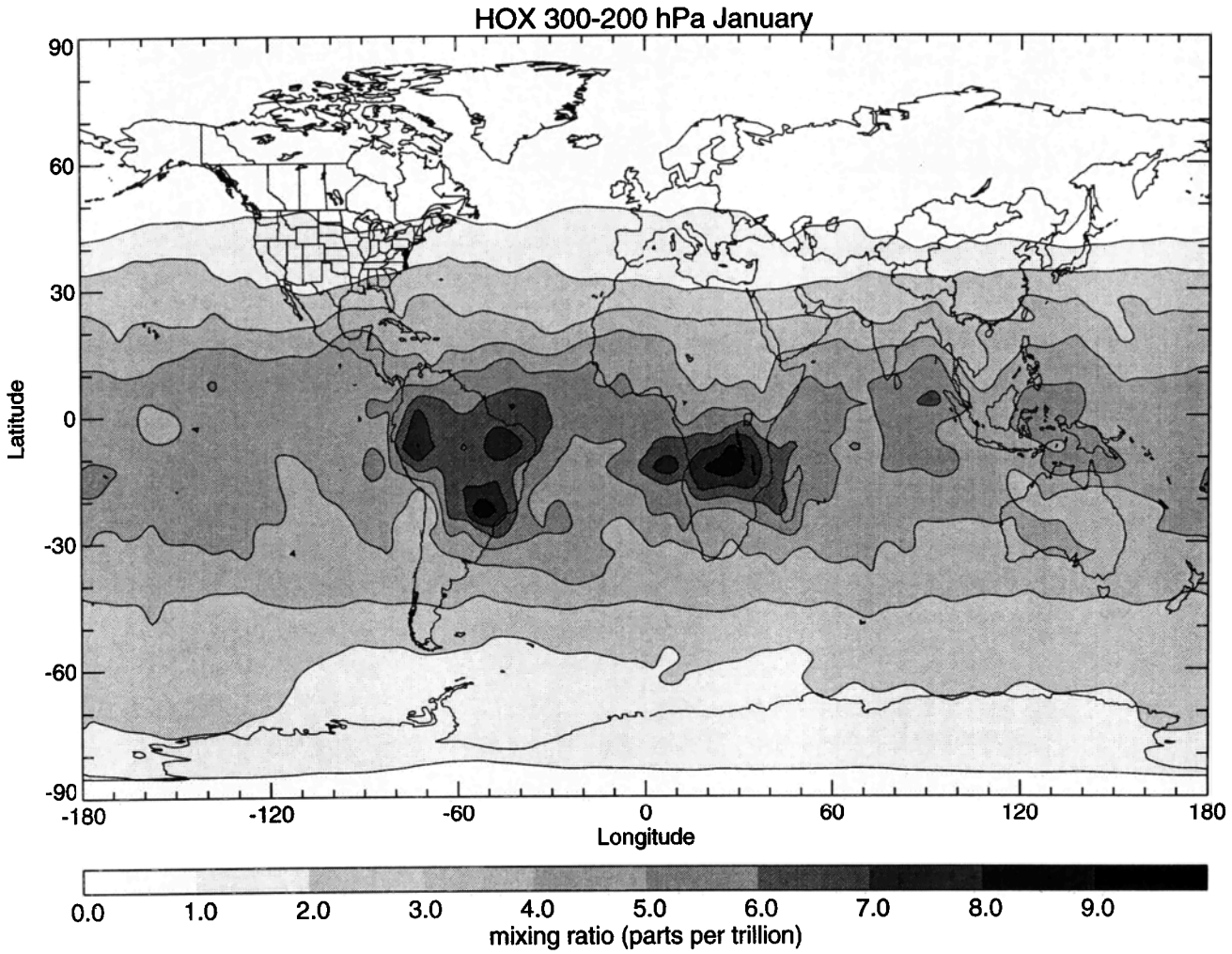

Figure 1. Monthly mean model January HO_x mixing ratios in ppt for 300–200 hPa.

gion 300–200 hPa. We will concentrate on this region rather than the 200-100 hPa region since it avoids the tropopause in the higher latitudes. There are significant HO_x maxima up to 9 ppt over the equatorial continental areas of South America and Central Africa. To understand this, we looked in detail at the HO_x production and loss fluxes (Figures 2 and 3). Here the reason for the HO_x maxima can be seen, since the HO_x maxima coincide with areas of large HO_x production through photolysis of the organic compounds, formaldehyde, acetone, methyl hydroperoxide, and methyl glyoxal. These compounds have strong surface sources in these areas from vegetation, so the hypothesis we wish to test is that they are lifted up to the upper troposphere by convection.

3.1. Comparison With Measurements

We have validated the model simulation of ozone and NO_x in the work of *Collins et al.* [1997]. The changes to the model since then, particularly the use of 6-hourly wind fields, have improved the simulation of these species. The most notable change is in summertime ozone over the continents. This used to be overpredicted and is now much improved. It may have been that using 18 day averaged wind fields caused the air to stagnate over the continents. Results from the present model for carbon monoxide, NO_x and ozone show reasonable agreement with other models and with observations. They can be seen in the work of *Kanakidou et al.* [1998a, b]. In this paper we wish to evaluate the modeling of organic species, especially those affecting the upper tropospheric HO_x budget. Figures 4, 5, 6, and 7 show comparisons between modeled and observed concentrations for some organic species and H_2O_2. The model seems to overpredict formaldehyde in the South Atlantic (Figure 4) compared to measurements. *Jacob et al.* [1996] were also unable to reconcile model calculations with the observations here. They suggested that there maybe some formaldehyde loss that was not accounted for, possibly on aerosol surfaces. Our modeled acetone concentrations are higher than observed by around a third, which is expected since our sources are unrealistically high. There is a large difference between the modeled and observed methyl hydroperoxide in the northern PEM-West B sites [*Talbot et al.*, 1997] (Figure 5). This might be because our sample of model data north of 20°N may include air masses with higher

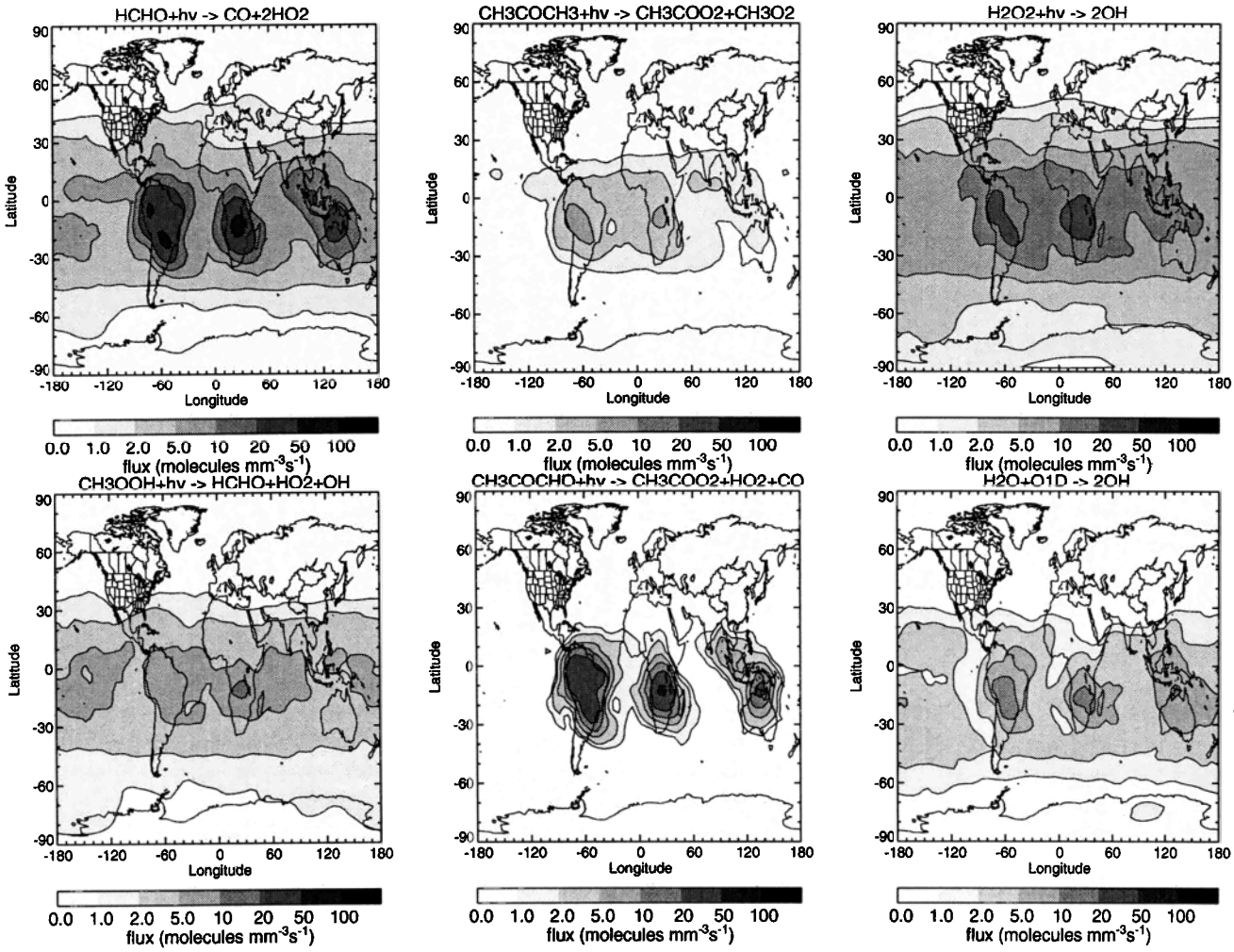

Figure 2. Monthly mean model January HO_x production fluxes in molecules mm^{-3} s^{-1} for 300–200 hPa.

concentrations that left Asia south of 20°N. In Figure 6 all three species at Mauna Loa increase in the model between September and January, whereas the observations show a decrease. The model correctly simulates the January to April concentration changes, but shows a decrease in all the species between April and July where the observations show an increase. The model concentrations over Hawaii seem to be very sensitive to the position of the inter-tropical convergence zone, and the convective wet removal associated with it. The latitudinal distribution of acetone in the west Pacific (Figure 7) shows reasonable agreement with observations. The acetone excesses in the model at 10°–0°S and 20°–30°N may be due to our overestimate of the acetone emissions from vegetation. Unfortunately, there are not sufficient measurements of isoprene and its reaction products to validate the isoprene chemistry in the model, especially in the upper troposphere.

Our methane lifetime due to OH removal is 9.6 years, in reasonable agreement with *Prinn et al.* [1995], who calculated a lifetime of 8.9±0.6 year. However, the methane lifetime (or the methyl-chloroform lifetime) only gives an indication of the OH concentration in the lower troposphere tropics. It is not useful for assessing the upper tropospheric HO_x concentrations.

It is difficult to compare modeled upper tropospheric HO_x with aircraft measurements since aircraft only make instantaneous measurements along the aircraft track. The HO_x concentration can have fine scale features (both temporally and spatially) that a global chemistry model will not capture. Another difficulty is created since we use meteorology from a climate integration of the GCM, rather than historical meteorology corresponding to the measurement periods. We have attempted to extract more detailed information on the HO_x concentrations in our model by outputting the instantaneous concentrations of any parcel that passes within 60 nautical miles (~ 111 km) of a specified location. These data are output every advection time step (3 hours). With such a small search radius the parcel density at each location is approximately 1 per 120 hPa (~ 1 per 4–5 km in the upper troposphere) so data are accumulated over a few months to get a representation of the height profile. Figure 8 shows two profiles, Figure 8a is of the OH concentration over Hawaii, and Figure 8b is of the OH and HO_2 mixing ratios over Fiji.

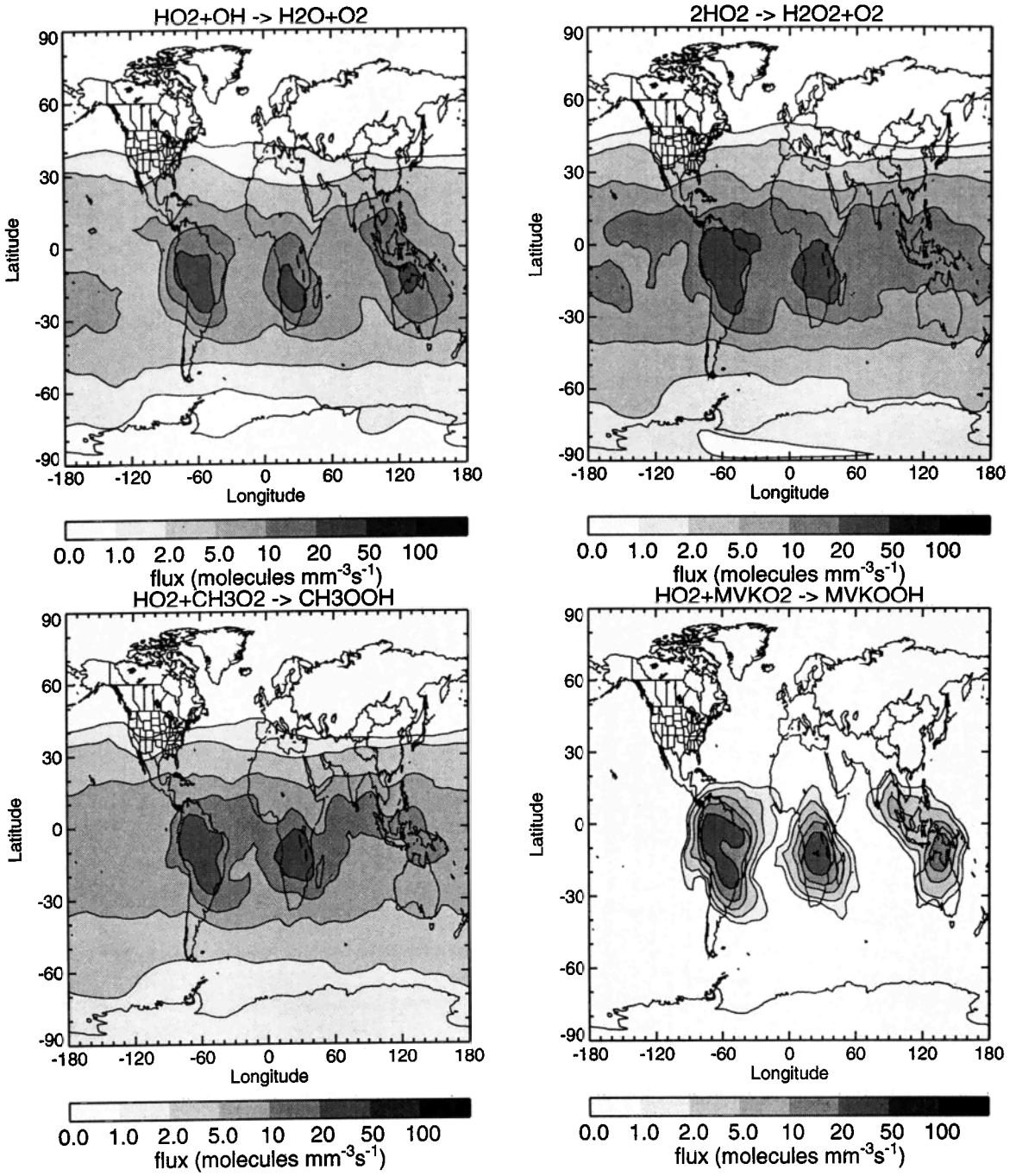

Figure 3. Monthly mean model January HO_x destruction fluxes in molecules mm^{-3} s^{-1} for 300–200 hPa.

Each symbol represents the instantaneous mixing ratio or concentration of one model parcel at one time step. The scales and units have been chosen to allow comparison with *Wennberg et al.* [1998, Figure 3] and *Folkins et al.* [1997, Figure 1]. The modeled results are certainly comparable with the observations, but their spread is too large to be able to determine whether the model is accounting for all the possible HO_x sources.

3.2. Effect of Convection

We have used our model to investigate the effect of convection by turning on our convective transport scheme for only selected species. Our control run had no convection, then six experiments had convection turned on separately for formaldehyde, acetone, hydrogen peroxide, methyl hydroperoxide, isoprene + products (MVK, isoprene hydroperoxide, MVK hydroperoxide, methyl glyoxal), and all species. These experiments were run for 5 months, from September through to January. The modeled upper tropospheric diurnally averaged HO_x concentrations with no convection are shown in Figure 9. Comparing this with Figure 1 shows that convection induces a very significant increase, particularly over the tropical continents. Here the increase in HO_x is around 50–60%. This experimental setup

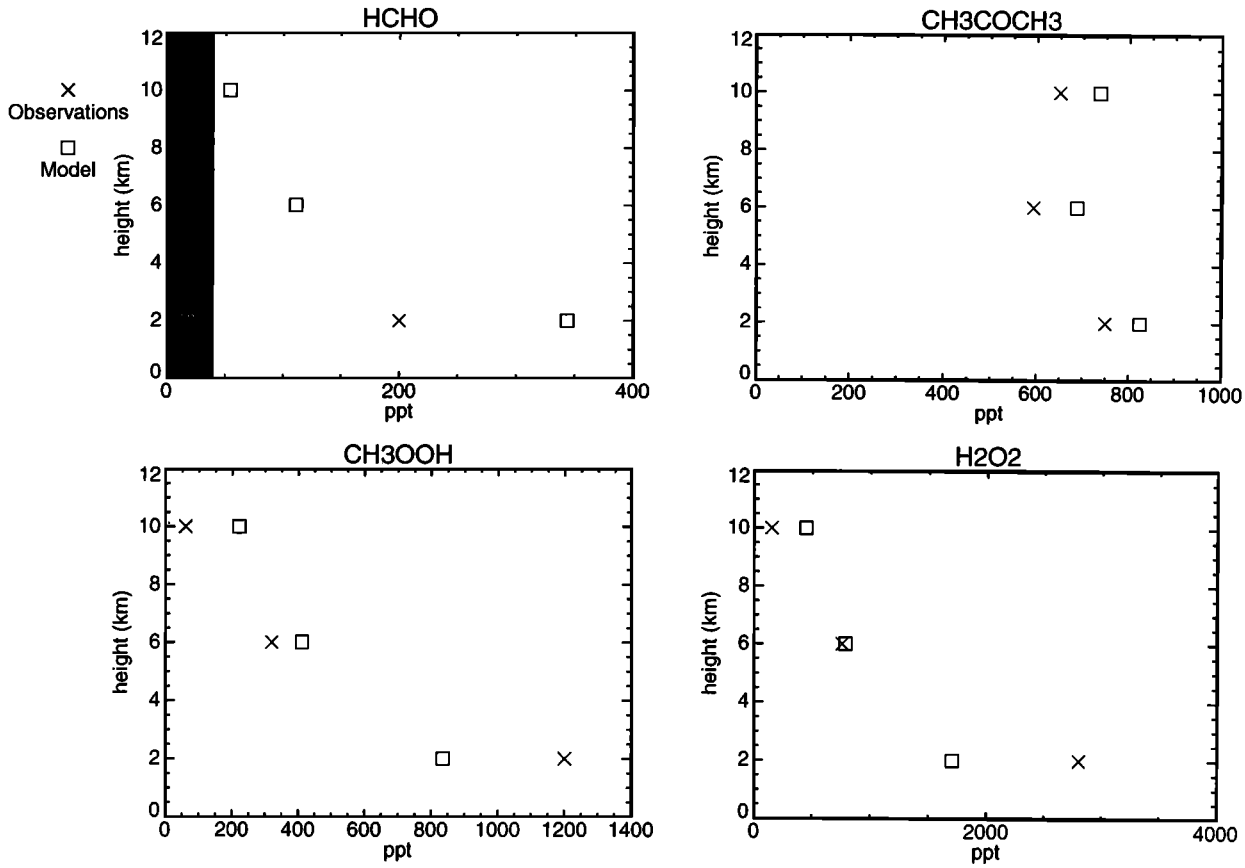

Figure 4. Comparison between model (squares) and observations (crosses) of some organic species over the South Atlantic in October. Observations are from *Jacob et al.* [1996]. Concentrations of HCHO below 40 ppt were below the detection limit of the observations.

whereby one species was convected at a time was chosen because it was the most conceptually simple. However, the control is a no convection atmosphere which is not realistic. Another approach might have been to take the fully convecting atmosphere with high upper tropospheric HO_x as the control and turn off the convection for one species at a time. Since the HO_x destruction is roughly quadratic in the radical concentrations, it might be expected that the HO_x increase due to the convection of each species would be slightly less in this case. However, the ranking of the species in terms of their effect on upper tropospheric HO_x should remain unchanged.

Table 4 shows the effects of convection of selected species on the HO_x budget in January. The first column of figures lists the fluxes through each reaction integrated over the whole 300–200 hPa region for the case with no convection. With no convection, the $O^1D + H_2O$ reaction is still a significant source of HO_x (8.3×10^3mols s^{-1}). Photolysis of hydrogen peroxide and formaldehyde, provide sources of similar magnitude (9.2 and 8.0 $\times10^3$mols s^{-1} respectively), however much of the hydrogen peroxide is formed in situ by the removal of two HO_2 radicals and so cannot be considered a true source. Similarly, although the two largest radical sinks are the formation hydrogen peroxide and methyl hydroperoxide (11.1 and 9.1 $\times10^3$mols s^{-1}) , these cannot be considered true sinks as most of the hydrogen peroxide, and about half of the methyl hydroperoxide are photolyzed back to radicals. The formation of water vapour from OH and HO_2 is a definite sink (9.0×10^3mols s^{-1}) and is probably the largest HO_x loss.

The next columns in Table 4 list the changes in the fluxes when each species is convected relative to the case with no convection. The convection of most of the species (acetone is the exception) increase the fluxes through photolysis of the hydroperoxides. Since none of the compounds lead to the hydroperoxides as reaction products, these do not generate net HO_x production except in the case of convection of the hydroperoxides themselves. Otherwise, the changes in these photolysis fluxes are due solely to the increased cycling of HO_x through the hydroperoxides caused by higher HO_x and RO_2 levels. The convection of ozone precursors has little effect on the $O^1D + H_2O$ reaction ($\leq +0.2\times10^3$mols s^{-1}). The only significant change is when ozone itself is subject to convection (right-hand column). This transports significant amounts of ozone out of the upper troposphere to lower altitudes.

Convection of isoprene and its products has the largest effect on the HO_x production. Although isoprene only

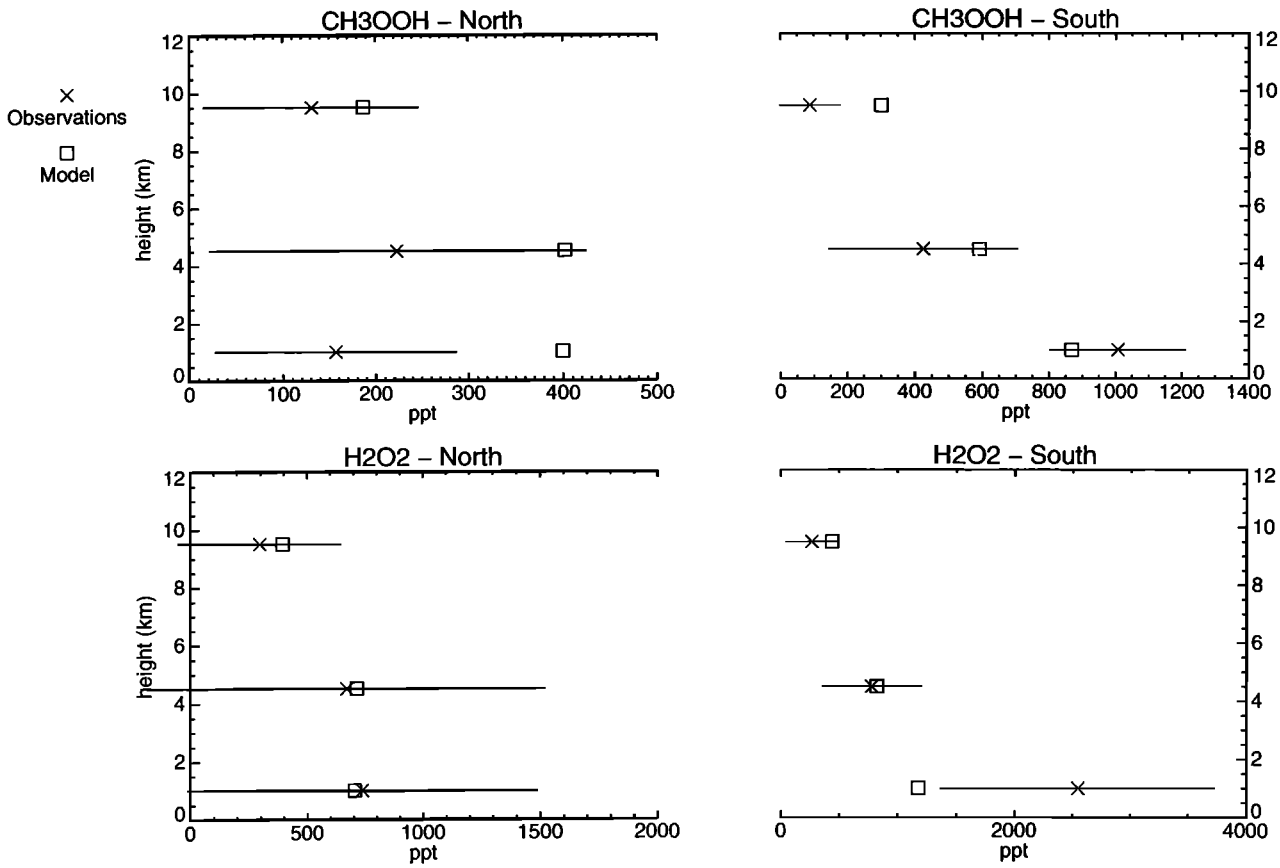

Figure 5. Comparison between model (squares) and observations (crosses) of hydrogen peroxide and methyl hydroperoxide over the western Pacific in February–March. Observations are from *Talbot et al.* [1997]. Error bars are one standard deviation. For the observations the data are divided according to whether the air masses left the Asian coast north or south of 20°N. For the modeled values the data are divided according to whether they are sampled north or south of this line.

has a lifetime of a few hours, its products such as MVK, the hydroperoxides of isoprene and MVK, and methyl glyoxal all live long enough to be convected to the upper troposphere. The major increase to the HO_x source seems to be through photolysis of methyl glyoxal ($+5.1\times10^3$mols s^{-1}), with formaldehyde photolysis also significant ($+3.5\times10^3$mols s^{-1}). The formation of hydroperoxides of isoprene and MVK is a radical sink since, compared to methyl hydroperoxide and hydrogen peroxide, these are attacked strongly by OH and have less chance to be photolyzed back to radicals. This offsets the production terms by 3.6×10^3mols s^{-1}.

The last row of Table 4 shows the relative increase in the amount of HO_x in the 300–200 hPa layer due to the convection of the different species. The values are normalized to give fractional increases. Convection of isoprene, hydrogen peroxide and methyl hydroperoxide cause the largest increases in HO_x (15, 14, and 13%, respectively). This is in spite of the hydroperoxides being subject to wet deposition in areas of convective rain. It should be noted that although convective transport for species is turned on and off for these experiments, the convective wet removal is still applied for all species in each experiment. Formaldehyde and acetone result in lesser HO_x increases (6% each) when convected. With the usual model configuration of convecting all species, upper tropospheric HO_x is increased by 52% compared to no convective transport.

The budgets have also been studied for the top layer of our model (200–100 hPa). The same qualitative remarks are true as for the 300–200 hPa region. With lower absolute reaction fluxes, the relative effect of convection is slightly larger at the higher altitudes.

4. Discussion

The effect of convecting acetone in our model seem to be less important on the upper tropospheric HO_x concentrations than convecting the other species considered here. This is because, even with emissions of 70 Tg yr^{-1}, the source strength for acetone is much less than for the others. This is compounded by the fact that acetone has a long lifetime (about a month) and is therefore moderately well mixed throughout the troposphere and less influenced by convection.

Formaldehyde has a very large source strength, equiv-

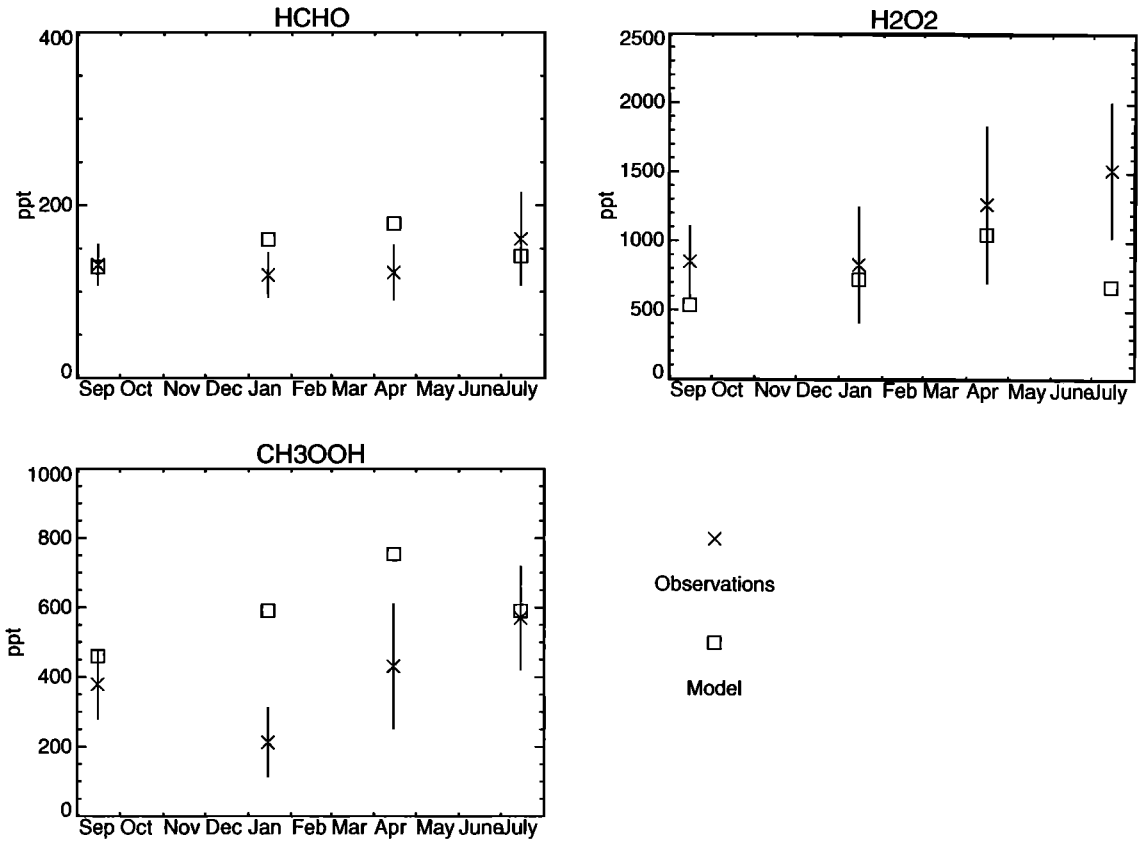

Figure 6. Comparison between model (squares) and observations (crosses) of species in downslope conditions at Mauna Loa. Model data are taken at a height of 3 km. Observations are from *Brasseur et al.* [1996]. Error bars are one standard deviation.

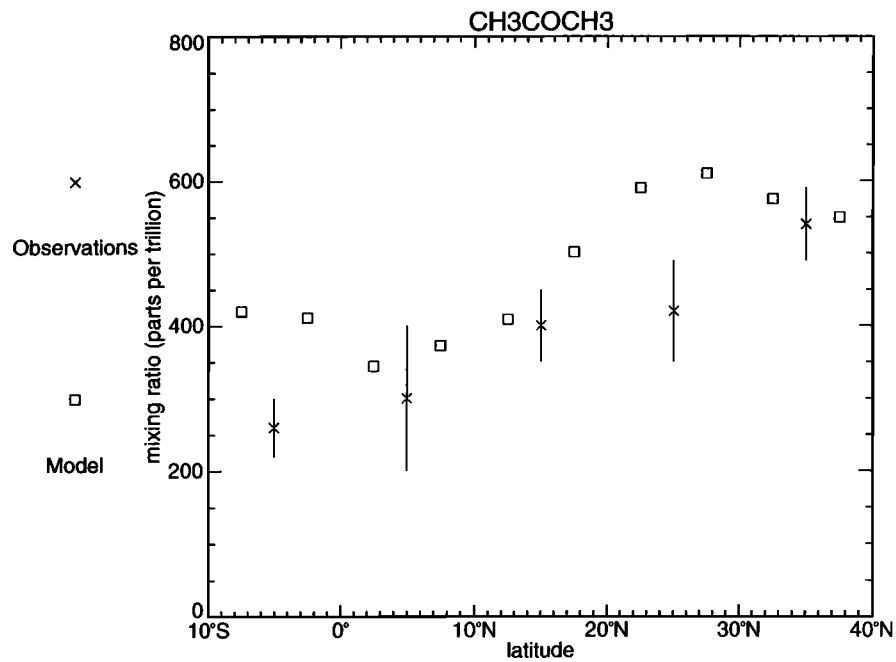

Figure 7. Comparison between modeled and observed acetone concentrations in the Pacific free troposphere (5–10 km) in February–March [*Singh et al.*, 1995]. Error bars are one standard deviation.

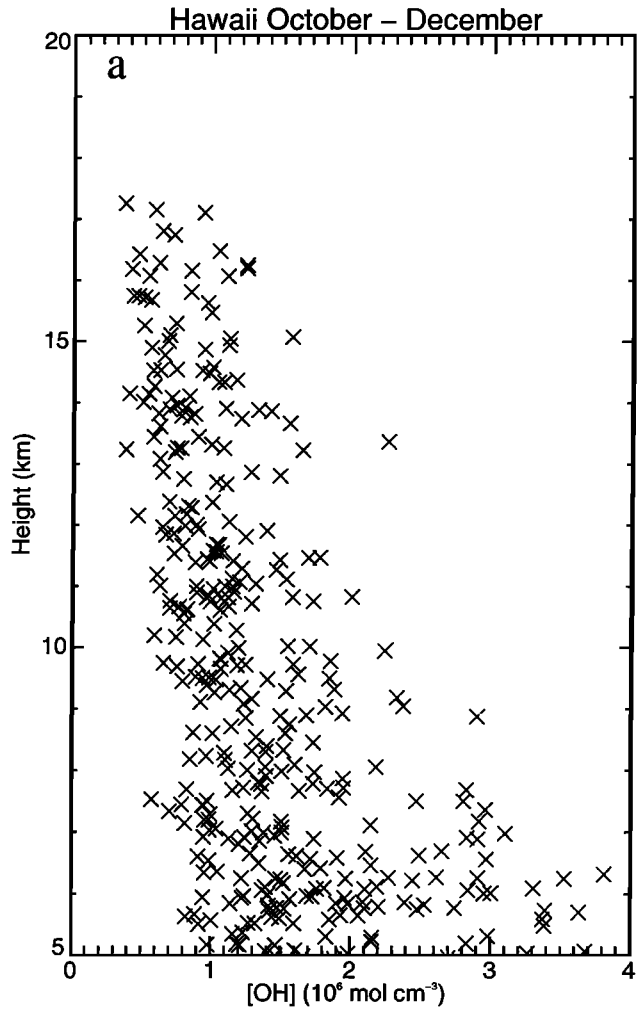

Figure 8. Profiles of (a) the OH concentration over Hawaii, combined data for 0000 and 2100 UTC from the months October to December, and (b) the OH (crosses) and HO_2 (squares) mixing ratios over Fiji, combined data for 0000, 0300, and 2100 UTC from the months September to November. Each symbol represents the instantaneous mixing ratio or concentration of one model parcel at one time step.

alent to around 1400 Tg yr^{-1} globally (mostly from methane oxidation). This is mainly from the lower tropospheric tropics, where methane is oxidized most strongly. Formaldehyde has a short lifetime of about 8 hours and so is not well mixed and has a strong vertical gradient, making it less abundant in the upper troposphere. However this vertical gradient is only slightly reduced by convection since, with such a short lifetime, the formaldehyde distribution is more dependent on in situ production than on transport. Convection has more effect on the formaldehyde distribution by transporting its precursors, especially those which (unlike methane) are attacked primarily by photolysis rather than OH radicals. Convection of formaldehyde does not increase the HO_x production from formaldehyde photolysis ($+2.1\times10^3$mols s^{-1}) by as much as when isoprene is convected ($+3.5\times10^3$mols s^{-1}). Only about a third of the formaldehyde in the upper troposphere is photolyzed to HO_2 radicals. Most of the rest produces H_2 or H_2O molecules.

Isoprene also has a large source (500 Tg yr^{-1}). It has a lifetime of only a few of hours so it has a very steep vertical gradient. With such a short lifetime though, it is not that susceptible to convection so we chose also to convect its degradation products. Some of its degradation products such as isoprene hydroperoxide and methyl vinyl ketone have longer lifetimes of around half a day, and these are readily transported to the upper troposphere by convection. Here the next stable degradation product methyl glyoxal is formed (4 hour lifetime). This is efficiently photolyzed giving a net gain of two radicals. At each stage in the degradation process a formaldehyde molecule is formed which can also photolyze to more radicals. If in reality the lifetimes of the isoprene degradation products we have neglected (such as methacrolein) were a lot less than for isoprene hydroperoxide and MVK, this would reduce the effect of isoprene convection on upper tropospheric HO_x.

Guenther et al. [1995] calculated the global VOC emissions from vegetation to be 1150 Tg yr^{-1}. These emissions are largest in the tropics where the growing season occurs at the time of greatest convective rainfall. This correlation between convective activity and VOC emission makes vegetation a potentially huge source of upper tropospheric HO_x. Along with our isoprene emissions, we have included only another 100 Tg yr^{-1} of VOC emissions from vegetation. If the missing 550 Tg yr^{-1} of emissions included species or degradation products which convection could transport to the upper troposphere, this might increase HO_x production still further.

The influences of the hydroperoxides (H_2O_2 and CH_3OOH) on the HO_x budget are less easy to quantify than the carbonyl photolysis. Although they have very large photochemical sources (roughly 10^3Tg yr^{-1} each), they are formed by the destruction of two radicals and so globally constitute a HO_x sink. Their influence on the upper tropospheric HO_x comes about when there is a net influx. Hydroperoxide production is second order in the radical concentrations, it is strongest in the tropics and increases with pressure. Hydrogen peroxide formation is catalyzed by water vapor and so is biased toward the surface. Methyl hydroperoxide production occurs particularly near surface sources of hydrocarbons although the HO_2+RO_2 reactions compete with the NO+RO_2 reaction and so peroxide production is negatively correlated with NO_x emissions. The above factors give the peroxides steep vertical gradients, with maxima just above the boundary layer (below the boundary layer they are destroyed by dry deposition). They have lifetimes of around a day, so convection readily transports them to the upper troposphere.

In Table 4, with no convection, the photolysis rate of hydrogen peroxide (9.2×10^3mols s^{-1}) is slightly less than its production rate (11.1×10^3mols s^{-1}). This implies that its large scale advective influx nearly offsets the other destruction processes (mainly wet deposition).

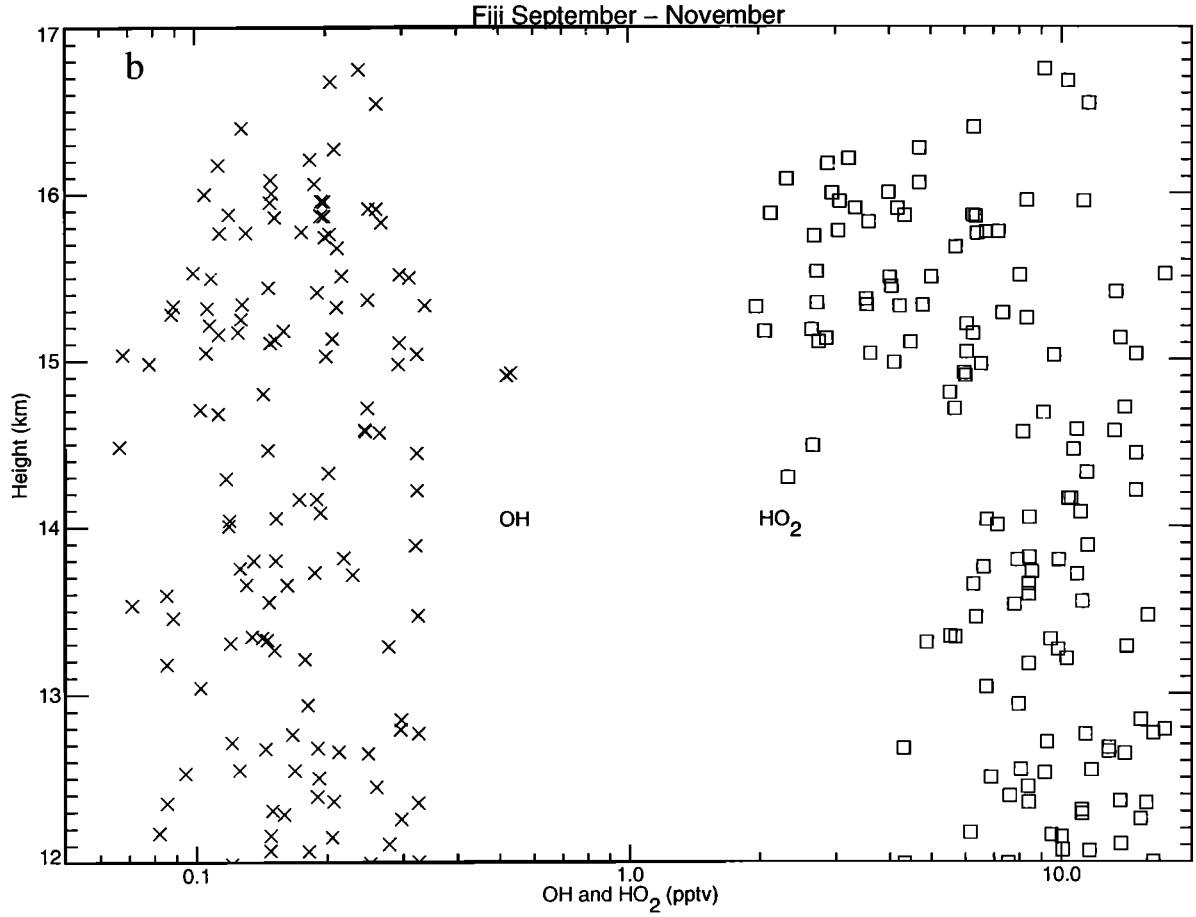

Figure 8. (continued)

When it is convected, the flux through the photolysis reaction increases by far more than the hydrogen peroxide production flux (+5.3 compared to $+1.7 \times 10^3$mols s^{-1}), giving a net HO_x gain. The photolysis flux of methyl hydroperoxide (4.3×10^3mols s^{-1}) is about half its production flux (9.1×10^3mols s^{-1}), implying that the large scale advection cannot make up for its other losses. The (nonphotolytic) loss of methyl hydroperoxide is larger than for hydrogen peroxide, since it is attacked more strongly by OH. Convecting methyl hydroperoxide increases the photolysis flux by more than it increases its production flux (+2.1 compared to $+1.5 \times 10^3$mols s^{-1}). Therefore, even though methyl hydroperoxide formation and destruction still constitutes a net loss of HO_x, this loss is less than for the case when methyl hydroperoxide is not convected. An additional HO_x increase ($+1.9 \times 10^3$mols s^{-1}) is generated from the extra formaldehyde produced from the methyl hydroperoxide degradation.

The contributions of the convection of individual species to the total upper tropospheric HO_x will not add linearly, since although the HO_x production rate is linear in the precursor concentrations, the destruction rate is quadratic in the radical concentrations. The change in total HO_x due to convection of all species (52%) is close to sum of the individual HO_x changes in the five species listed in Table 4 (54%). This is probably a coincidental cancellation between the effects of the nonlinear chemistry and the convection of extra species such as the nonmethane hydrocarbons and NO_x.

Our convection scheme is fairly simple in that it mixes material evenly over a vertical column. A more realistic model might entrain material at the cloud base, detrain it at the top, and have a general subsidence connecting the two. This would enhance the effect of convection in our simulations even further, as it would be more efficient still at moving material from near the surface to the upper troposphere. Our wet deposition scheme removes material evenly (as a function of height) from every Lagrangian parcel within a grid square with convective precipitation. The effect of convection might be less if the wet removal was concentrated only on those parcels participating in the convection. This would affect hydrogen peroxide the most, but have a small effect on formaldehyde, methyl hydroperoxide, isoprene hydroperoxide, and MVK hydroperoxide. The scavenging coefficients for these last two are not well known. The molecules do contain an OH group but would have to be a factor of 10 more soluble than methyl hydroperoxide to significantly reduce the effect of isoprene on the upper tropospheric HO_x.

We varied our experiment by reducing the fraction of a grid square subject to convective wet removal to 0.05 (roughly the fraction of a grid square that is cov-

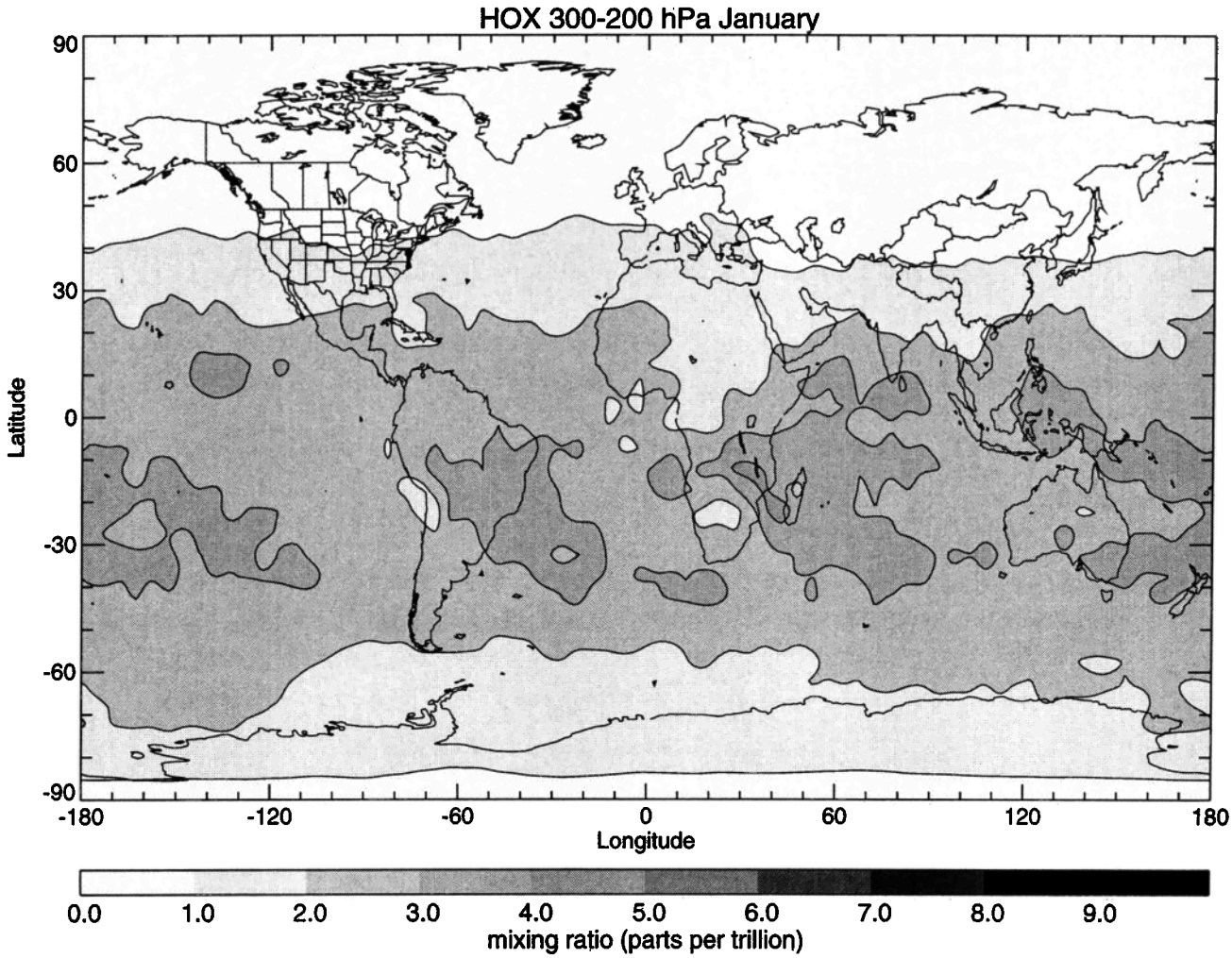

Figure 9. Monthly mean model January HO_x mixing ratios in ppt for 300–200 hPa with no convection.

Table 4. Reaction Fluxes for the Region 300–200 hPa

Reaction	Convected Species						
	None	HCHO	CH_3COCH_3	H_2O_2	CH_3OOH	C_5H_8[a]	All
			Production Terms				
$HCHO + h\nu$	8.0	+2.1	+0.6	+0.5	+1.9	+3.5	+8.4
$CH_3COCH_3 + h\nu$	2.1	+0.0	+0.5	+0.0	+0.0	+0.0	+0.5
$H_2O_2 + h\nu$	9.2	+0.8	−0.3	+5.3	+0.9	+1.8	+10.1
$CH_3OOH + h\nu$	4.3	+0.1	−0.2	+0.3	+2.1	+1.0	+3.9
$CH_3COCHO + h\nu$	0.3	+0.0	+0.0	+0.0	+0.0	+5.1	+5.0
$H_2O + O^1D$	8.3	+0.2	+0.2	+0.2	+0.2	+0.0	−0.7
			Destruction Terms				
$HO_2 + OH$	9.0	+1.1	+1.1	+2.8	+1.7	+1.1	+4.5
$HO_2 + HO_2$	11.1	+1.2	−0.4	+1.7	+1.6	+2.7	+9.5
$HO_2 + CH_3O_2$	9.0	+0.5	−0.1	+1.4	+1.5	+3.0	+7.2
$HO_2 + (OH)MVKO_2$	0.3	+0.0	+0.0	+0.0	+0.0	+3.6	+3.8
			Concentration				
Normalized $[HO_x]$	1.00	+0.06	+0.06	+0.14	+0.13	+0.15	+0.52

Columns with convected species are differences with respect to the column for no convected species. Units are kmol s^{-1}.

[a] Includes the larger oxidation products from isoprene.

ered by the convective precipitation) rather than 0.3. This doubled the upper tropospheric hydrogen peroxide concentrations (so disagreeing with observations), making hydrogen peroxide photolysis the most important source of upper tropospheric HO_x. The HO_x production through photolysis of the other species increased too, leading to a 20% overall increase in upper tropospheric HO_x concentrations. This shows how sensitive these studies are to the implementation of wet removal schemes. *Prather and Jacob*, [1997] remove 75% of the convected hydrogen peroxide which would further reduce its influence on upper tropospheric HO_x.

In this study we have investigated the effect of convecting species which can be directly photolyzed to produce HO_x radicals. NO_x is not one of these, but it is worth discussing the effect it has on HO_x chemistry. In the upper troposphere the largest convective source of NO_x in our model is from lightning in convective clouds rather than convective transport itself. In NO_x time series for points in the upper troposphere we see large spikes in the concentration reaching 10–100 times the background concentrations and lasting a few hours. These are similar to those observed by *Brunner et al.* [1998] and are probably caused by convection. The very high concentrations will certainly dominate the HO_x destruction through reaction (4) for a short time over a small area, but when spatially and temporally averaged, NO_x contributes only a few percent of the total January HO_x sink in the 300-200 hPa region. NO_x also affects HO_x destruction by increasing the OH/HO_2 ratio and hence increasing the importance of the HO_2+OH reaction relative to HO_2+HO_2. Through ozone production, NO_x can increase the HO_x production by ozone photolysis. All these processes probably have more relevance for studies on upper tropospheric ozone [*Flatøy and Hov*, 1997] but would make NO_x convection an interesting subject for further study.

We have only studied the effects of convective transport for January conditions. At this time of the year, the zone of maximum convective activity is located south of the equator. This has emphasized the influence of the biogenic emissions from the forests of South America and Central Africa. It would be very interesting to compare this with a July scenario. In this month the convective and photochemical activity extends as far north as the midlatitude industrial regions of North America, Europe, and Southeast Asia. Over these regions there are still substantial sources of biogenic emissions, but these are mixed in with large sources of anthropogenic nonmethane hydrocarbons, the convection of which may also play a significant role in the budget of upper tropospheric HO_x. The industrial regions have much higher surface sources of NO_x than the tropical forests in the wet season. This is likely to reduce the concentration of both biogenic and anthropogenic peroxides in the industrial boundary layer (and hence their convective contribution to the upper tropospheric HO_x budget) since many of the peroxy radicals will react with NO rather than with each other.

5. Conclusions

Convective transport increases HO_x by over 50% in the 300–200 hPa region. This can be largely accounted for by the convection of the five precursors considered in section 3.2. Convection of isoprene and its degradation products is the most important direct HO_x source, through methyl glyoxal and formaldehyde photolysis. Although hydrogen peroxide and methyl hydroperoxide are not direct HO_x sources, they act as HO_x temporary reservoirs enabling HO_x to be convected from its lower troposphere source region to the upper troposphere. Formaldehyde and acetone convection have a significant effect on upper tropospheric HO_x concentrations, but much less than the other species considered.

The major uncertainties in this work are the model convection scheme, the lack of coupling of convective wet deposition to convective transport, and the isoprene oxidation scheme. While changes to any of these will change the detailed numbers, we think it unlikely that they would change the qualitative conclusions. The exception might be a change in the relative importance of hydrogen peroxide and isoprene. We are aware that we rely heavily on our model for our conclusions and hope that soon upper tropospheric measurements of relevant species, particularly the isoprene oxidation products, will be able to confirm or refute these conclusions. Either way we have shown that convection has a profound effect on upper tropospheric HO_x and is an area worthy of further study.

Acknowledgments. We are grateful to the U.K. Department of Environment, Transport and the Regions, for its help and encouragement through contracts EPG 1/3/93 (Air Quality Division) and PECD 7/12/37 (Global Atmosphere Division).

References

Brasseur, G.P., D.A. Hauglustaine, and S. Walters, Chemical compounds in the remote Pacific troposphere: Comparison between MLOPEX measurements and chemical transport model calculations, *J. Geophys. Res., 101,* 14,795–14,813, 1996.

Brune, W.H., et al., Airborne in situ OH and HO_2 observations in the cloud-free troposphere and lower stratosphere during SUCCESS, *Geophys. Res. Lett., 25,* 1701–1704, 1998.

Brunner, D., J. Staehelin, and D. Jeker, Large-Scale nitrogen oxide plumes in the tropopause region and implications for ozone, *Science, 282,* 1305–1309, 1998.

Carter, W.P.L., and R. Atkinson, Development and evaluation of a detailed mechanism for the atmospheric reactions of isoprene and NO_x, *Int. J. Chem. Kinet., 28,* 497–530, 1996.

Collins, W.J., D.S. Stevenson, C.E. Johnson, and R.G. Derwent, Tropospheric ozone in a global-scale three-dimensional Lagrangian model and its response to NO_x emission controls, *J. Atmos. Chem., 26,* 223–274, 1997.

Crutzen, P.J., Photochemical reactions initiated by and influencing ozone in the unpolluted troposphere, *Tellus, 26,* 47–57, 1974.

Crutzen, P.J., and J. Fishmann, Average concentrations of

OH in the troposphere and the budgets of CH_4, CO, H_2, and CH_3CCl_3, *Geophys. Res. Lett., 4,* 321–324, 1977.

Crutzen, P.J. and P.R. Zimmerman, The changing photochemistry of the troposphere, *Tellus, 43,* 136–151, 1991.

DeMore, W.B., S.P. Sander, D.M. Golden, R.F. Hampson, M.J. Kurylo, C.J. Howard, A.R. Ravishankara, C.E. Kolb, and M.J. Molina, Chemical kinetics and photochemical data for use in stratospheric modeling, Evaluation number 11, *JPL Publ., 94-26,* 1994.

Derwent, R.G., and A.R. Curtis, Two-dimensional model studies of some trace gases and free radicals in the troposphere, *AERE-R8853,* Her Majesty's Stn. Off., London, 1977.

Flatøy, F., and Ø. Hov, NO_x from lightning and the calculated chemical composition of the free troposphere, *J. Geophys. Res., 102,* 21,373–21,381, 1997.

Folkins, I., P.O. Wennberg, T.F. Hanisco, J.G. Anderson, and R.J. Salawitch, OH, HO_2, and NO in two biomass burning plumes: Sources of HO_x and implications for ozone production, *J. Geophys. Res., 102,* 13,291–13,299, 1997.

Guenther, A., et al., A global model of natural volatile organic compound emissions, *J. Geophys. Res., 100,* 8873–8892, 1995.

Jacob, D.J., and S. C. Wofsy, Photochemistry of biogenic emissions over the Amazon forest, *J. Geophys. Res., 93,* 1477–1486, 1988.

Jacob, D.J., et al., Origin of ozone and NO_x in the tropical troposphere: A photochemical analysis of aircraft observations over the South Atlantic Basin, *J. Geophys. Res., 101,* 24,235–24,250, 1996.

Jaeglé, L., et al., Observed OH and HO_2 in the upper troposphere suggests a major source from convective injection of peroxides, *Geophys. Res. Lett., 24,* 3181–3184, 1997.

Johns, T.C., R.E. Carnell, J.F. Crossley, J.M. Gregory, J.F.B. Mitchell, C.A. Senior, S.F.B. Tett, and R.A. Wood, The second Hadley Centre coupled ocean-atmosphere GCM: Model description, spinup and validation, *Clim. Dyn., 13,* 103–134, 1997.

Kanakidou, M., et al., 3-D global simulations of tropospheric CO distributions — Results of the GIM/IGAC intercomparison 1997 exercise, *Chemosphere* in press, 1998a.

Kanakidou, M., et al., 3-D global simulations of tropospheric chemistry with focus on ozone distributions — Results of the GIM/IGAC intercomparison 1997 exercise, *Eur. Comm. Rep.,* Eur. Comm., in press, 1998b.

Kasibhatla, P.S., H. Levy, W.J. Moxim, and W.L. Chameides, The relative impact of stratospheric photochemical production on tropospheric NO_Y levels: A model study, *J. Geophys. Res., 98,* 18,631–18,636, 1993.

Lelieveld, J., and P.J. Crutzen, Role of deep cloud convection in the ozone budget of the troposphere, *Science, 264,* 1759–1761, 1994.

Levy, H., Normal atmosphere: Large radical and formaldehyde concentrations predicted, *Science, 173,* 141–143, 1971.

Mahlman, J.D., H. Levy, and W.J. Moxim, Three-dimensional tracer structure and behaviour as simulated in two ozone precursor experiments, *J. Atmos. Sci., 37,* 65–685, 1980.

Martinez, R.D., A.A. Buitrago, N.W. Howell, C.H.G. Hearn, and J.A. Joens., The near UV absorption spectra of several aliphatic aldehydes and ketones at 300 K, *Atmos. Environ., Part A, 26,* 785–792, 1992.

Paulson, S.E., and J.H. Seinfeld, Development and evaluation of a photooxidation mechanism for isoprene, *J. Geophys. Res., 97,* 20,703–20,715, 1992.

Penner, J.E., C.S. Atherton, J. Dignon, S.J. Ghan, J.J. Walton, and S. Hameed, Tropospheric nitrogen: A three-dimensional study of sources, distributions, and deposition, *J. Geophys. Res., 96,* 959–990, 1991.

Penner, J.E., C.S. Atherton, and T.E. Graedel, Global emissions and models of photochemically active compounds, in *Global Atmospheric Biospheric Chemistry,* edited by R.G. Prinn, pp. 223–247, Plenum, New York, 1994.

Prather, M.J., and D.J. Jacob, A persistent imbalance in HO_x and NO_x photochemistry of the upper troposphere driven by deep tropical convection, *Geophys. Res. Lett., 24,* 3189–3192, 1997.

Prinn, R.G., R.F., Weiss, B.R. Miller, J. Huang, F.N. Alyea, D.M. Cunnold, P.J. Fraser, D.E. Hartley, and P.G. Simmonds, Atmospheric trends and lifetime of CH_3CCl_3 and global OH concentrations, *Science, 269,* 187–192, 1995.

Singh, H.B., D. O'Hara, D. Herlth, W. Sachse, D.R. Blake, J.D. Bradshaw, M. Kanakidou, and P.J. Crutzen, Acetone in the atmosphere: Distribution, sources, and sinks, *J. Geophys. Res., 99,* 1805–1819, 1994.

Singh, H.B., M. Kanakidou, P.J. Crutzen, and D.J. Jacob, High concentrations and photochemical fate of oxygenated hydrocarbons in the global troposphere, *Nature, 378,* 50–54, 1995.

Stevenson, D.S., W.J. Collins, C.E. Johnson, and R.G. Derwent, Intercomparison and evaluation of atmospheric transport in a Lagrangian model (STOCHEM), and a Eulerian model (UM), using ^{222}Rn as a short-lived tracer, *Q. J. R. Meteorol. Soc. , 125,* 2477–2493, 1998.

Stockwell, W.R., F. Kirchner, M. Kuhn, and S. Seefeld, A new mechanism for regional atmospheric chemistry modeling, *J. Geophys. Res., 102,* 25,845–25,879, 1997.

Talbot, R.W., et al., Chemical characteristics of continental outflow from Asia to the troposphere over the western Pacific Ocean during February–March 1994: Results from PEM-West B. *J. Geophys. Res., 102,* 28,255–28,274, 1997.

Walton, J.J., M.C. MacCracken, and S.J. Ghan, A global-scale Lagrangian trace species model of transport, transformation, and removal processes, *J. Geophys. Res., 93,* 8339–8354, 1988.

Wennberg, P.O., et al., Hydrogen radicals, nitrogen radicals, and the production of O_3 in the upper troposphere, *Science, 279,* 49–53, 1998.

Zimmerman, P.R., R.B. Chatfield, J. Fishman, P.J. Crutzen, and P.L. Hanst, Estimates on the production of CO and H_2 from the oxidation of hydrocarbon emissions from vegetation, *Geophys. Res. Lett., 5,* 679–682, 1978.

W. J. Collins, R. G. Derwent, C. E. Johnson, D. S. Stevenson, Hadley Centre for Climate Prediction and Research, Meteorological Office, London Rd, Bracknell, Berks, RG12 2SZ, United Kingdom. (e-mail: wjcollins@meto.gov.uk; rgderwent@meto.gov.uk; cjohnson@meto.gov.uk; dstevenson@meto.gov.uk)

(Received November 5, 1998; revised February 22, 1999; accepted March 4, 1999.)